REVIEWS OF APPLIED ELECTROCHEMISTRY 23

Particle size and structural effects in platinum electrocatalysis

S. MUKERJEE

Tata Energy Research Institute, 7 Jor Bagh, New Delhi-110 003, India

Of the several factors which influence electrocatalytic activity, particle size and structural effects are of crucial importance, but their effects and mechanism of interaction, *vis-a-vis* overall performance, have been, at best, vaguely understood. The situation is further aggravated by the use of a wide range of experimental conditions resulting in non-comparable data. This paper attempts systematically to present the developments to date in the understanding of these structural interactions and to point out areas for future investigation. The entire content of this review has been examined from the context of the highly dispersed Pt electrocatalyst, primarily because it has been examined in the greatest detail. In the first two sections a general idea on the correlations between surface microstructure and geometric model is presented. Subsequently, indicators of a direct correlation between particle size and catalyst support synergism are considered. The structural and particle size effect on electro-catalysis is examined from the point of view of anodic hydrogen oxidation and cathodic oxygen reduction reactions. The hydrogen and oxygen chemisorption effects, presented with the discussion on the anodic and cathodic electrocatalytic reactions, provide important clues toward resolving some of the controversial findings, especially on the dependence of particle size on the anodic hydrogen oxidation reaction. Finally, the effect of alloy formation on the cathodic oxygen reduction reaction is discussed, providing insights into the structural aspect.

1. Inroduction

Highly dispersed noble metals (platinum and platinum alloys) on high surface area supports such as carbon blacks, are currently the most favoured electro-catalysts for applications in phosphoric acid fuel cell systems. Commensurate with the development of these electrocatalysts, numerous studies have been made to understand the structural and particle size effects on their electrocatalytic activity. Electron microscopic studies way back in the 1940s and 50s have proved that supported catalysts possess a crystal-line structure, dispelling the earlier conjectures of amorphicity. However, in practice, catalysts are never uniform, and exhibit particle size distribution, lattice defects (Frenkel or Schottky) and dislocations. The following questions then arise: are all lattice surfaces equally active? Do surface clusters of particles and surface atoms have comparable activity? Does catalytic activity depend on particle size? Is there an optimal particle size or distribution?

In the past decade, several studies have been carried out to answer these questions and most of them have resulted in widely differing and often contradicting results, mainly due to differences in catalyst prepara-tion, electrode pre-treatments, cell operating con-ditions and different analytical and interpretative methods. The aim of this review is to provide a better insight into this field and to present some of the latest work in this area, so as to offer some definitive answers to the above questions.

2. Surface structure of small particles

Well defined geometric models simulating the relation-ship between the particle size and population of crystal-lographic surface sites associated with atoms at edges, vertices, and low index crystal planes can provide important clues into the dependence on particle size. However, an accurate representation of the structure of a small catalyst particle through a well defined geometric model is debatable. Therefore, it is unrealistic to expect a metallic supported catalyst to contain particles with the exact number of atoms necessary to yield a structure corresponding to a particular geome-tric model. Hence, for a more realistic model, one must assume that (a) the shape of the particles are such that their free energy is at a minimum, (b) atoms in excess of that required to form a complete geometric structure are located at the crystal sites which produce a particle as nearly spherical as possible. Using these two assumptions as principles in developing a mathe-matical model, Hardeveld and Montfoort [1] have presented an interesting correlation in accounting for the IRspectra of N_2 on Ni, Pd and Pt. This showed the presence of an appreciable fraction of surface sites with coordination number five (the so called B_5 sites) on metal particles in the range 1.5–7.0 nm. Using the
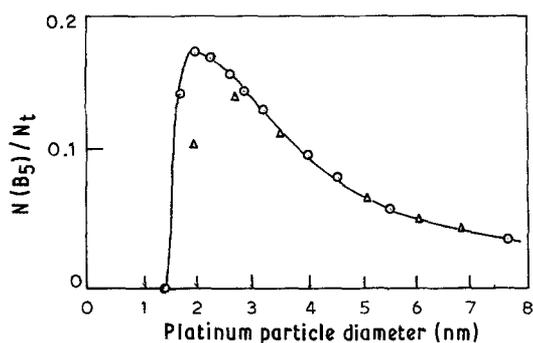
Fig. 1. Relative fraction of B_5 sites present on Pt particles with octahedron (O) and cubo-octahedron (△) structure.

Table 1. Dependence of coordination number on crystallite size for a Pt face-centred cubic structure

Crystallite length ($\mathring{A}$)	Number of atoms	Average coordination number
5.5	2	4.0
8.5	3	6.0
13.8	5	4.5
27.5	10	8.3
49.5	18	8.6
137.5	50	8.9

mathematical analysis of Hardeveld and Montfoort [1], Kinoshita [2] determined the variation in the fraction of B_5 sites ($N(B_5)/Nt$), as a function of platinum particles in the shape of an octahedron and cubo octahedron (Fig. 1). A maximum for B_5 sites occurs for ~ 2 nm diameter particles and for platinum particles with diameters < 1.5 nm or > 8.0 nm the fraction of B_5 sites is small. Furthermore, as the platinum particle size approaches > 8.0 nm it nearly approximates to a sphere with predominantly (1 1 1) and (1 0 0) platinum crystal planes. The ratio Hs/Nt (defined as the fraction of surface atoms obtained from chemisorption of hydrogen assuming one hydrogen atom (Hs) chemisorbed per surface metal atom [3–5], to the total number of atoms on the surface (Nt)) and the active metal surface area of platinum [6] shows that for Hs/Nt to be 0.5, the platinum surface area must be greater than 140 m^2 g^{-1} corresponding to a particle size of 2.5 nm (Fig. 2). Extrapolating further, it also implies that at a particle size of 1.0 nm almost every atom in the particle becomes a surface atom (that is, at Hs/Nt $= 1$). However, for a particle size of this magnitude, the 'metallic character' found in bulk may no longer exist.

The dependence of coordination number on particle size (shown in Table 1) indicates an appreciable change in coordination number and hence in activity for particle size below 4.0 nm. Although this correlation is based on a model lattice [7], similar correlation with other models does not alter this figure substantially [8].

At this juncture, it is also essential to take into account the fact that measurement techniques for estimation of platinum particle size are many and varied, each with their associated pros and cons. Amongst the more widely used techniques are chemisorption with CO of H_2, either via first adsorbing and then measuring the desorbed gas, or via progressive surface titration of pre-adsorbed oxygen on platinum with H_2 at room temperature.

Cautious handling is essential when applying the first method because problems, such as overestimation of surface area of supported metals, are likely to arise in catalysts exhibiting hydrogen spillover. On the other hand, an accurate idea of the stoichiometry between the active metal and the chemisorbed gas is essential in the second method. This is, however, complicated due to the variance of stoichiometry with particle size.

Electrochemical techniques, on the other hand, have problems associated with the surface re-arrangements and roughening caused by potential cycling, as shown by the LEED studies on platinum monocrystal [9]: these affect the reproducibility and the precision of measurement. The X-ray diffraction line broadening method is another technique which can be used for particle size measurements. However, the range of measurements possible is between 5.0–100 nm diameter for supported catalyst. For smaller crystallites, the width of the diffraction line profile due to crystallite size is very broad and not discernible above the background. Electron microscopy (both DFEM and BFEM) is among the other well known methods for characterization of platinum particle size. Accuracy in the application of this method depends on the defocus conditions, and hence on the elevation of the particle in the supported sample with respect to the plane of focus.

Finally, possible changes in electrical conductivity of supported electrocatalysts with crystallite size should be investigated, since these changes can effect charge transfer.

3. Microstructure of highly dispersed platinum catalyst and its interaction with carbon support

3.1. Microstructure

Before discussing the microstructure of supported platinum electrocatalysts, a brief examination of the
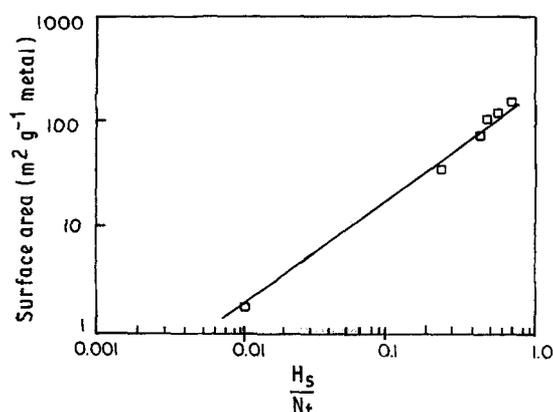

Fig. 2. Relationship between surface area and fraction of surface atoms on particles of noble metals determined by hydrogen chemisorption [6] for Pt metal atoms.

methods used to prepare them is called for. The most widely accepted techniques for preparation of such supported catalysts are by the adsorption of colloidal metal particles on the support. The colloidal 'sols' are generally prepared by the chemical reduction of a suitable salt of the noble metal (such as $H_2PtCl_6 \cdot xH_2O$). Depending on the reaction conditions such as choice of reducing agents, medium of reduction, concentration of the platinum metal salt, pH of the solution etc., particle sizes ranging from 50-1.5 nm can be realized. One of the most widely accepted techniques in this regard is the sulphur colloid technique [10, 11], by which a very high degree of dispersion with average particle size in the region of 1.5-3.5 nm can be realized. Heat treatment at 900° C in an atmosphere of nitrogen causes the platinum particles to grow to a uniform particle size of mean value 4.2 ± 0.5 nm with fairly normal distribution. This heat treatment also causes uniform distribution of platinum over the carbon particles. Since the cubic lattice parameters in the heat treated catalysts is found to be in excellent agreement with that expected in bulk platinum ($a = 0.3918$ nm), platinum crystallites are essentially single crystals [12]. Furthermore, a previous study by Jalan et al. [13] using ultra high resolution electron micrographs has shown that platinum crystallites of around 4.0 nm size are very thin (raft like, disc like, or two dimensional). This was arrived at from a side view of platinum microcrystallites at the outer boundaries of the support carbon blacks (see Fig. 3) and was found to be 0.5-0.7 nm (two or three atom layers).

These thin particles are very much in contrast to the widely assumed spherical shapes used in model calculations. This may provide an explanation for the discrepancies in particle size measurements using X-ray line broadening and chemisorption techniques. The relevance of such findings to practical fuel cell electrocatalyst is that flat particles could provide greater ratio of surface atoms to total platinum atoms as compared to spherical particles. In addition, greater surface stresses are expected, which would indicate a different intrinsic activity vis-a-vis bulk surface.
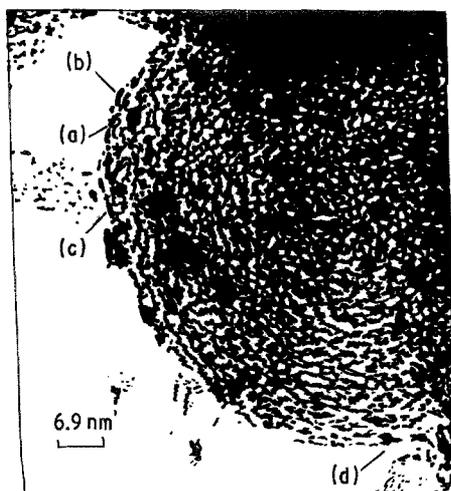
Besides, greater interaction with support carbon black would be expected.

3.2. Catalyst-support synergism

Electronic interaction and synergistic effects between catalyst and the support has been established by conventional catalytic and electrochemical studies. Electron-spin resonance (ESR) studies, for example, have demonstrated electron donation by platinum to the carbon support [14]. This is further supported by X-ray photoelectron spectroscopy studies [15] showing the metal acting as an electron donor to the support, their interaction depending on the Fermi-level of electrons in both. Bogotski et al. [16] have attempted to account for the change in electrocatalytic activity due to catalyst support synergism on the basis of changes in the electronic state of Pt when deposited on the carbon support. According to them, the electrical double layer formed between the microdeposit (platinum) and the support is indicated, to a certain extent, by the difference in the electronic work functions of platinum (5.4 eV) and the carbon support (pyrolytic graphite 4.7 eV), thereby resulting in an increase of electron density on the platinum. However, the rise in electron density can be significant only if particle size of the microdeposit (platinum) is comparable to the thickness of the double layer. The dependence of particle size to thickness of the double layer had been illustrated by Kobelev et al. [17] who have shown that if the change in electron density is assumed to occur in a layer 0.3 mm thick and the platinum microdeposits are in the shape of a tetrahedron with edge 'a', the ratio of the double layer volume to the volume of the whole microdeposit amounts to 71, 42, 28, and 21% for 'a' equal to 0.6, 1.0, 1.5 and 2.0 nm, respectively. Hence, the particle size of the catalyst metal crystallite does influence the catalyst support synergism.

4. Structural effects on electrocatalysis

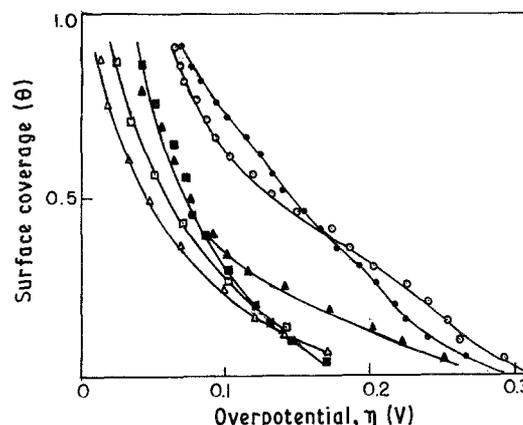As a result of the use of supported noble metal (notably platinum) electrocatalyst in low temperature

Fig. 3. Electron micrograph of 10 w/o Pt on Vulcan XC-72 showing thin Pt micro particles.

Fig. 4. Dependence micrograph of surface coverage on potential for hydrogen adsorption on Pt(●), Pd(O), Ir(▲), Rh(■), Ru(□) and Os(△) in H_2SO_4.

acid fuel cell electrodes (both for anodic and cathodic reactions), numerous studies have been directed towards determining its sensitivity to the particle size and other structural effects *vis-a-vis* its specific activity or turnover frequency (site time yield). A study of the effects of particle size on catalysis of supported metals, however, requires a definition of particle size. In general, particle size is defined as the average value determined from metal surface area measurements (chemisorption and progressive surface poisoning studies), X-ray line broadening analysis, or electron microscopic measurements [3]. The effects of these structural features on the chemisorption and electrocatalytic activity at the hydrogen and oxygen electrodes will be discussed in this section.

4.1. Hydrogen chemisorption

Since hydrogen atoms participate in electrocatalytic reductions and in fuel cell anodic oxidation, some hydrogen adsorption features shall be presented here. The results of the detailed examination of classical adsorption have, however, been presented elsewhere [18–20]. Polycrystalline platinum, palladium and iridium show two major peaks for hydrogen during potential sweep on the positive potential region [21], indicative of multiple adsorption states. The surface coverage on this group of metals varies almost linearly with the potential (Fig. 4) [21, 22]. Single crystal studies with platinum using potential sweep methods [20, 23–25] show multiple adsorption states existing in all three main crystallographic planes $\langle 1\,0\,0\rangle$, $\langle 1\,1\,0\rangle$, $\langle 1\,1\,1\rangle$ (Fig. 5). This potentio-dynamic sweep technique has been applied in numerous studies to examine the quasi-equilibrium adsorption isotherms of hydrogen on platinum. Kinoshita and Stonehart [26, 27] have obtained potentio-dynamic profiles for hydrogen deposition and oxidation on a series of high surface
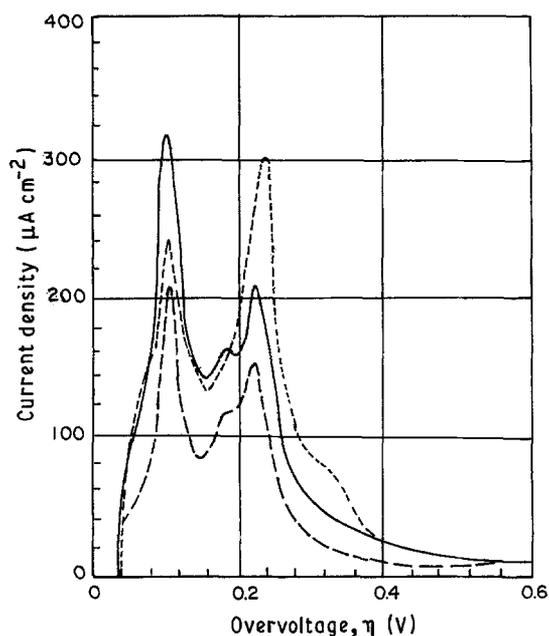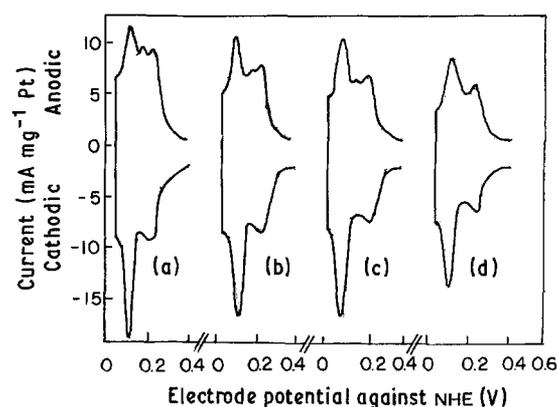
Fig. 6. Potentiodynamic current potential profiles for hydrogen deposition and oxidation on 1.37 mg, Pt electrocatalyst supported on graphitized carbon [26, 27], 1 M H_2SO_4, 23°C, sweep rate of $0.015\,V\,s^{-1}$: (a) 64; (b) 57; (c) 52; (d) 42; $m^2\,g^{-1}$ Pt.

area platinum electrocatalysts (2.8–480 nm particles) in 1 M H_2SO_4.

According to their data presented in Fig. 6, Kinoshita and Stonehart have shown that the cathodic deposition current-potential profiles do not change with platinum particle size, whereas the anodic oxidation profiles do. The distinguishing feature of these current potential profiles is the presence of a third anodic peak located at an electrode potential between 'strongly' and 'weakly' adsorbed hydrogen peaks, which becomes more pronounced as the surface area increases (particle size decreases). This third peak is, however, not observed in the cathodic current potential profiles. For a platinum electrocatalyst with a surface area of $69\,m^2\,g^{-1}$ (4.2 nm particle diameter), deconvolution analysis of current potential peaks have shown that the surface coverage associated with the third anodic peak accounts for about 14% of the total hydrogen coverage. The variation in the anodic profiles with different platinum surface areas was correlated to a change in the relative concentrations of surface atoms identified with edges, vertices, and crystal faces. Using the cubo-octahedron structure as their geometric model for platinum particles, Kinoshita and Stonehart have concluded that the weakly and strongly bonded adsorbed hydrogen species are associated with $\langle 1\,1\,1\rangle$ and $\langle 1\,0\,0\rangle$ crystal faces, respectively and that the third anodic peak is associated with adsorbed hydrogen on edge atoms of platinum particles.

Besides the above finding, Angerstein-Kozlowska et al. [28] have shown the existence of induced surface heterogeneity in $\langle 1\,0\,0\rangle$ and $\langle 1\,1\,1\rangle$ planes of single crystal platinum in H_2SO_4. This surface heterogeneity is supposed to arise on each plane or edge because of different coordination numbers for the various metal atoms, which would result in a different 'environment' for the adsorbate at each metal site. For instance, atoms at the corners of a $\langle 1\,1\,1\rangle$ plane for f.c.c. platinum have a coordination number of 4, while those at the edges and on the face have a coordination number of 7 and 9, respectively [7]. Therefore, as the length of the crystallite edge increases, the coordination number of surface atoms varies (Table 1).
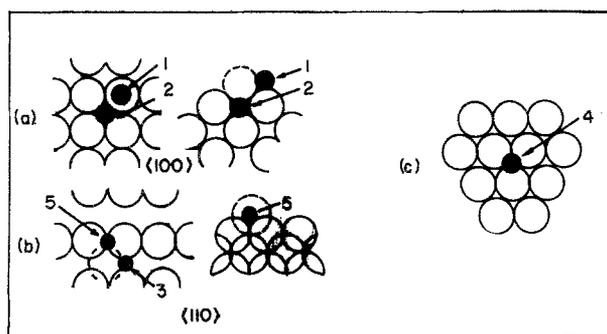
Fig. 5. Hydrogen adsorption on three main crystallographic planes of Pt [24].

Fig. 7. Positions for adsorbed hydrogen on a face-centred cubic metal lattice: (a) 1, 2 on the $\langle 1\,0\,0\rangle$ face, (b) 3 and 5 on the $\langle 1\,1\,0\rangle$ face, (c) 4, the single position on the $\langle 1\,1\,1\rangle$ face.

Thus, a dependence of activity to crystallite size is anticipated. The conclusion of Kinoshita and Stonehart [26, 27] have been supported by more recent studies carried out by Ross et al. [9, 23, 29], Yeager et al. [30, 31] and Hubbard et al. [32]. These studies were carried out using LEED, AES and electrochemical techniques to show convincingly that the oxidation and deposition of adsorbed hydrogen on single crystal platinum electrodes in acid electrolytes is different in $\langle 1\,1\,1\rangle$ and $\langle 1\,0\,0\rangle$ faces. Qualitative interpretation of these single crystal results have been attempted by Shopov et al. [33] (Fig. 7) in his calculations of hydrogen adsorption on f.c.c. nickel. The positions 3–5 for $\langle 1\,1\,0\rangle$ and $\langle 1\,1\,1\rangle$ faces are grouped in the 'weaker' bonded form and the positions 1 and 2 of the $\langle 1\,0\,0\rangle$ face are grouped in the 'stronger' bonded form.

4.2. Oxidation of molecular oxygen

The mechanism for electrochemical oxidation of molecular hydrogen over polycrystalline platinum in acid electrolyte involves slow dissociation of adsorbed hydrogen molecules to hydrogen atoms [34, 35] (known as Tafel reaction), followed by fast electrochemical oxidation of the adsorbed hydrogen atoms to protons (known as the Volmer reaction):

$$H_2 + 2M \longrightarrow 2MH \quad \text{(Tafel)}$$

$$2MH \longrightarrow 2M + 2H^+ + 2e^- \quad \text{(Volmer)}$$
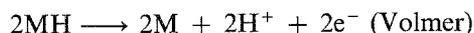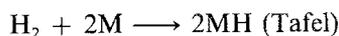
Ross and Stonehart [34] and Vogel et al. [35], in their investigations on electrochemical oxidation of hydrogen molecules on platinum in H_2SO_4, H_3PO_4, over smooth platinum, platinum black and platinum-supported on carbon have found no dependence of platinum particle size down to 3.0 nm. The latter investigation involved a combination of cyclic voltammetry and potentiostatic techniques in both H_2SO_4 and H_3PO_4 electrolytes. In addition, it was inferred that since hydrogen dissociation is the rate-determining step and since hydrogen dissociation takes place only on the platinum (not on the carbon support), 'hydrogen spillover' from platinum to the carbon substrate should not influence the rate of hydrogen oxidation [36]. These observations [35] have been contradicted by

Urrison et al. [37], whose result on smooth and highly dispersed platinum ($180\,\mathrm{m}^2\,\mathrm{g}^{-1}$ Pt) on carbon support in solution with a pH ranging between 0.4 to 15.6 have a difference of 1.5 to 2 orders of magnitude in favour of the highly dispersed platinum on carbon support. In addition, dependence of exchange current density on platinum surface area was reported with a fourfold increase caused by a change in platinum surface area from 26 to $51\,\mathrm{m}^2\,\mathrm{g}^{-1}$. Discrepancies between the results of Urrison et al. and Vogel et al. can be accounted for on the basis of several factors. The principle reason could be the difference in carbon support surface areas ($180\,\mathrm{m}^2\,\mathrm{g}^{-1}$ in case of Urrison et al. as compared to $80\,\mathrm{m}^2\,\mathrm{g}^{-1}$ for Vogel et al.). This could result in different degrees of catalyst support synergisms.

4.3. Oxygen chemisorption

Despite a detailed investigation of oxygen adsorption and reduction, controversy still exists due to the widely varying, non-standardized techniques and surface pretreatments which have different effects on the slow oxygen electrosorption. This section will deal with some aspects of oxygen chemisorption, with special emphasis on the structural aspects and models proposed.

Depending on the potential, oxygen is bound on the surface of the noble metal electrocatalyst as a chemisorbed species or as a surface oxide. For most transition metals such as palladium or platinum, the formation of these surface oxygen layers is independent of the presence of oxygen and is irreversible. Hence, reductive removal of these oxygen layers is a slow kinetic process commencing at potentials well below the characteristic potential for layer formation on each metal surface.

As in the case of hydrogen, platinum is the most well-studied electrocatalyst. Optical measurements [38–40] show that a freshly developed oxygen layer on platinum behaves reversibly up to 0.95 V. However, rapid aging of OH is assumed to occur in this potential range [39, 40] formed by

$$S^* + H_2O \longrightarrow [OH]_s + H^+ + e^- \quad (1)$$
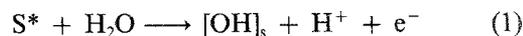
where S^* is the number of sites occupied by the surface species. Three different OH species have been proposed by Conway et al. [40, 41] with $S^* = 1, 2,$ and 4 formed in successive reactions. Irreversible layers arise from the reaction of [OH] to form [O], which can lead to oxide growth [39, 41].

$$[OH] \longrightarrow [O] + H^+ + e^- \quad (2)$$
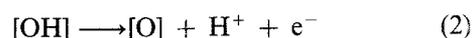
Above 1.0 V, a platinum-oxygen species is formed which, upon cathodic potential sweep, reduces to platinum in one step, without forming an [OH] intermediate [40].

While a clearer picture exists for oxygen binding on metal surfaces at highly anodic potentials, the oxygen layer in the low potential regime deserves attention. The latter prevails in oxygen reduction in fuel cells etc.
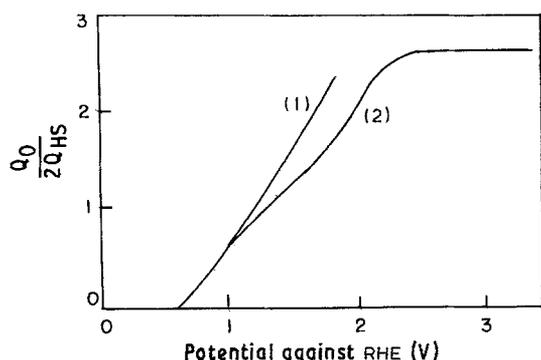
Fig. 8. Oxygen electrosorption with potential curves 1 and 2 for Pt [44, 45].

The surface coverage-potential curves for platinum and palladium exhibit an inflection at about 1.0–1.5 V (Fig. 8) [42, 43], corresponding to a surface monolayer of oxygen atoms (PtO) formed via Reactions 1 and 2.

This structure is attributed to surface oxide formation on platinum and palladium 0.9 V and up to 1.5 V, where PtO_2 and PdO_2 are also formed [46, 47]. The linearity of these coverage-potential plots (Fig. 8) can be attributed to either activated chemisorption [39, 40, 48, 49] or oxide kinetics [44]. Although the latter would not predict a limited surface coverage, this is possible if oxide formation becomes transport-limited after the formation of a saturated surface oxide monolayer. In view of the preliminary evidence on the surface species presented above, the characterization of the surface layer as chemisorbed oxygen more likely.

Irreversible adsorption under induced surface heterogeneity (Elovich equation) can explain both steady state and transient surface coverage results with surface species arising from Reactions 1 and 2. Surface heterogeneity has been observed by Conway and co-workers [40] for oxygen species electrosorption on platinum anodes. Three oxygen states were identified below a monolayer of OH on platinum, possibly resulting from hybrid bonding and exchange on the surface. While some investigators interpret their
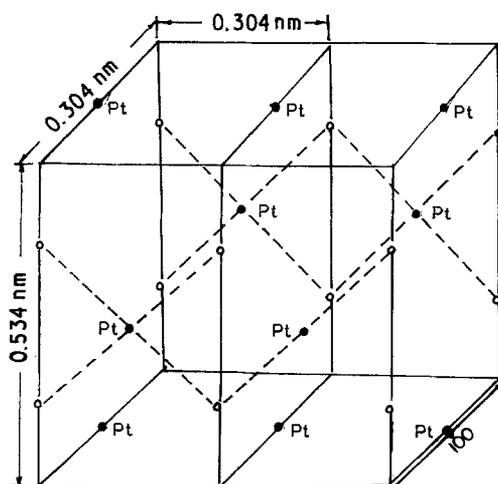

Fig. 9. Lattice structure of bulk PtO; (o) Pt atoms; (●) O atoms [50].
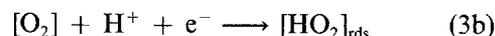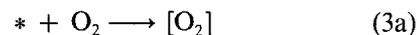
results as indicative of chemisorption or oxygen dissolution in the lattice or under the surface, others propose oxide formation of stoichiometry PtO or PtO_2 [50, 51]. Fig. 9 shows a possible structure of platinum oxides on various planes [50]. The $\langle 1\,0\,0 \rangle$ plane has a PtO_2 composition [50, 51], while the bulk corresponds to a PtO oxide. The present information does not clearly indicate either surface oxide formation or chemisorption. Coordinated efforts using standardized techniques and procedures are essential to resolve these uncertainties.
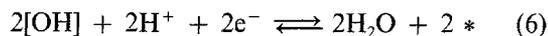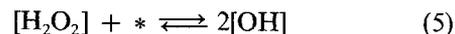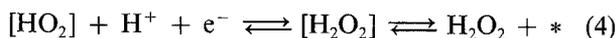
4.4. Reduction of molecular oxygen

Based on the present evidence, the 'peroxide radical' mechanism [29, 52, 53] seems to best explain molecular oxygen reduction in both acidic and basic solutions. According to this mechanism, oxygen reduction in acid involves a concerted rate limiting step, between O_2 and H^+, with simultaneous electron transfer [52].

$$* + O_2 + H^+ + e^- \longrightarrow [HO_2]_{rds} \qquad (3)$$

or

$$* + O_2 \longrightarrow [O_2] \qquad (3a)$$

$$[O_2] + H^+ + e^- \longrightarrow [HO_2]_{rds} \qquad (3b)$$

This is followed by the formation of [OH] and $[H_2O_2]$ with possible desorption of the latter.

$$[HO_2] + H^+ + e^- \rightleftharpoons [H_2O_2] \rightleftharpoons H_2O_2 + * \qquad (4)$$

$$[H_2O_2] + * \rightleftharpoons 2[OH] \qquad (5)$$

$$2[OH] + 2H^+ + 2e^- \rightleftharpoons 2H_2O + 2* \qquad (6)$$

Since steps (4–6) are in quasi-equilibrium and follow the r.d.s., they are not proven mechanistic paths. However, evidence of H_2O_2 in solution [54] and the presence of surface (OH) discussed previously, support this mechanism. Kinetic evidence is consistent with this mechanism, assuming Temkin adsorption on oxygen-free platinum surfaces at low potentials < 1 V [52]. This mechanism holds for polycrystalline [55, 56] as well as single crystal platinum $\langle 1\,0\,0 \rangle$ and $\langle 1\,1\,1 \rangle$ [29]. The surface appears to be uniformly active for oxygen reduction, although reaction intermediates are adsorbed more strongly on steps than on flat surfaces [55]. Several surface species are known to compete for catalytic sites; however, the adsorption characteristics of $[HO_2]$ appear to predominate and result in the observed kinetic parameters [52].

Despite the fact that extensive investigations have been carried out on the reduction of oxygen on platinum in acids and bases, very few studies have been undertaken on their possible structural sensitivity. Even those investigations that were carried out have been fraught with initial controversies due to widely varying conditions, such as electrocatalyst support, preparative techniques, preconditioning, experimental conditions, etc.

One of the first investigations towards elucidating particle size and structural dependence was by Zeliger

[57] and Bett et al. [58]. Both these studies concluded that platinum atoms at the vertices, edges kink sites or dislocations are not more active than atoms on platinum crystal faces and hence specific activity for oxygen reduction is independent of platinum particle size. This conclusion was despite the fact that Zeliger's investigation involved platinum supported on asbestos while Bett et al.'s investigation was on commercial platinum blacks and platinum supported on graphitized carbon (average particle size between 3.0 and 40 nm; corresponding to surface areas between 96–6 m^2 gm^{-1}). In addition to this, both investigations were conducted at room temperature (20° C). Further support to this conclusion was provided by the investigations of Gruver [59] and Vogel et al. [60] who concluded similar independence of particle size on ORR (oxygen reduction reaction) activity. Furthermore, Kunz and Gruver [59] concluded that interactions between carbon and platinum were not significant since activity of smooth platinum and platinum-supported on carbon (70 m^2 g^{-1}) were found to be approximately the same in both 96% H_3PO_4 at 160° C and 20% H_2SO_4 at 70° C.

On the other hand, Blurton et al. [61] and Bregoli [62] found a decrease in specific activity for oxygen reduction with diminishing particle size from 12 nm to 3.0 nm and 2.0 nm respectively. Blurton et al. [61], in their studies on highly dispersed platinum on carbon in 20% H_2SO_4 at 70° C, attributed this effect to either a difference in the platinum particle size or an influence of the support on the platinum activity, or a combination of both these factors. Bregoli's study [62] involved highly dispersed platinum on carbon electrocatalyst in 99% H_3PO_4 at 177° C. He found the specific activity for oxygen reduction to vary by a factor of 2 in the range of particle size studied (12 nm to 2.0 nm). This conclusion was reached by an analysis of data presented in Fig. 10 where the solid line represents the experimental data. These conflicting conclusions regarding the effect of platinum particle size have been somewhat allayed by the investigations of Peuckert et al. [63], in their investigations on oxygen reduction activity of highly dispersed platinum on carbon in 0.5 M H_2SO_4. The platinum crystallite size studied ranged from around 1.0 nm to 12 nm (corresponding to 5 w/o Pt/c to 30 w/o Pt/c and 10 w/o Pt-black/c).
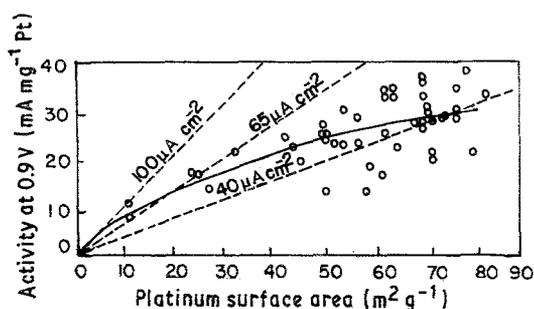

Fig. 11. Specific current density (mA cm^{-2} Pt) and turnover numbers (e$^-$/surface Pt atom) for dioxygen reduction in 0.5 M H_2SO_4 at 298 K as a function of average platinum crystallite size.

Activity measurements for electrochemical reduction of dioxygen in the form of site time yield (turnover frequency) on this series of platinum catalysts showed a constant site time yield for platinum particles larger than 4.0 nm. However, as the particle size decreased to around 1.0 nm the site time yield decreased twentyfold (Fig. 11).

It was also inferred that as the metal dispersion is increased, a larger fraction of platinum atom participate in surface reactions. However, since activity per surface atom decreases (as indicated by Peuckert et al.), an optimum particle size is indicated as the result of these two effects. As shown in Fig. 12, the maximum activity per unit weight of platinum is between 3.0–5.0 nm [63].

The decrease in the site time yield for oxygen reduction can now be seen as consistent with the previous study of the platinum particle size effects on the rate of oxygen reduction. Bett et al. [58] did not see an effect of particle size for catalysts with platinum

Fig. 10. Oxygen reduction activity of Pt electrocatalysts in 99% wt H_3PO_4 at 177° C as a function of platinum surface area [62]. (O) Pt supported on Vulcan XC-72, (□) Pt black mixed with Vulcan XC-72: (——) data fit; (— — —) constant specific activities.
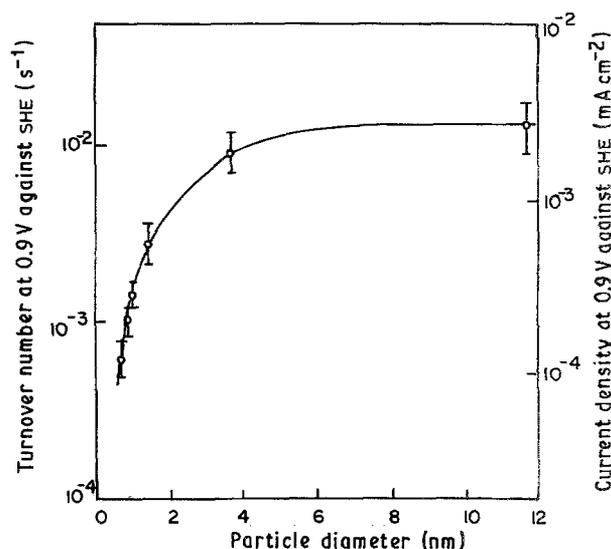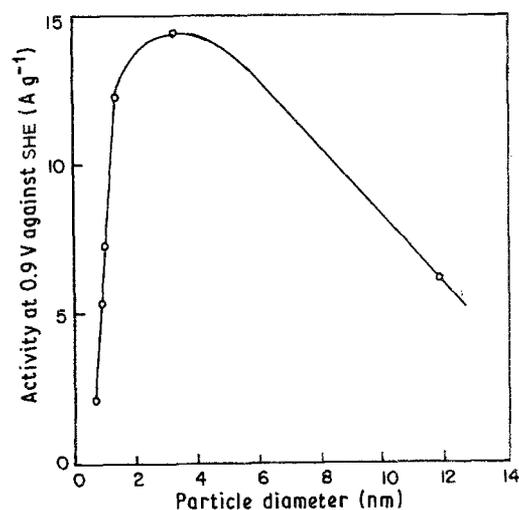

Fig. 12. Catalyst efficiency, expressed as current at 0.9 V against SHE per mass of platinum, as a function of average particle diameter.
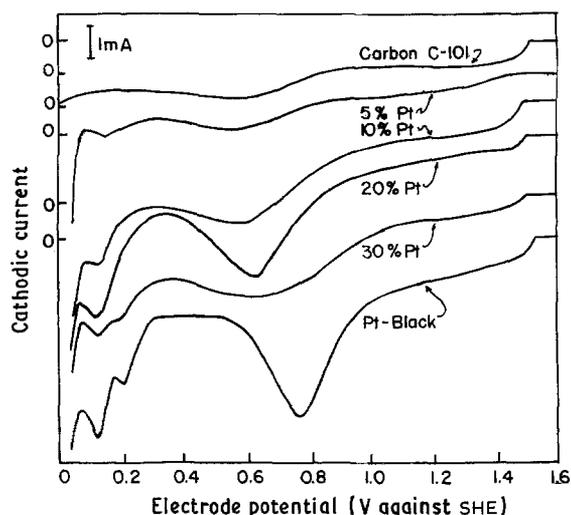
Fig. 13. Cathodic branches of cyclic linear sweep voltammograms of nitrogen purged carbon support and platinum carbon catalysts (scan rate: $0.1\ V s^{-1}$)

Fig. 14. The volcano plot for oxygen reduction in 8 M phosphoric acid showing concentration of Pt–Ru alloys (expressed in atom per cent).

crystallites larger than 3.0 nm. Bregoli [62] covered particle size range from 25.0 nm to 3.0 nm and reported a two-fold decrease in areal activity. Blurton *et al.* [61] covered the range between 1.7 nm to 10.0 nm and found a twenty-fold decrease in activity. The last two reports show greater scatter of data.

Peuckert *et al.* explained his results on the basis of an increase in the concentration of surface metal sites with low coordination number to other metal atoms. This interpretation was partly based on that of Ross *et al.* [50] who found no difference in ORR activity on platinum ⟨1 0 0⟩, platinum ⟨1 1 1⟩ and stepped platinum surface (containing a large fraction of surface sites with coordination number 7). This cause of the structure sensitivity may be associated with the strength of adsorption of the surface oxide species as indicated by the data in Fig. 13 showing the shift of oxide reduction wave with decrease in particle size. This has been ascribed to an increased heat of adsorption of the oxygen intermediate at low coordination surface metal sites. It is also interesting to note that the particle size range where the areal activity decreases rapidly corresponds to the size regimes where room temperature adsorption of dioxygen changes from PtO to Pt_2O. Further speculation, however, awaits a more detailed characterization of the metal surface during oxygen reduction.

4.5. Structural effects on electrocatalytic properties of platinum alloys

Recent studies on the alloying of platinum with base transition metals such as V, Cr, Si, Ti etc. have shown significant increase in the electrocatalytic activity towards the cathodic oxygen reduction reaction [64–66]. These studies were carried out on electrodes with gas diffusion geometry and under actual PAFC working conditions of (150–200° C temperature and 85–100% H_3PO_4). The Pt–Cr alloys were found to be the most active and stable amongst these binary alloys [66]. Several attempts have since been made to correlate
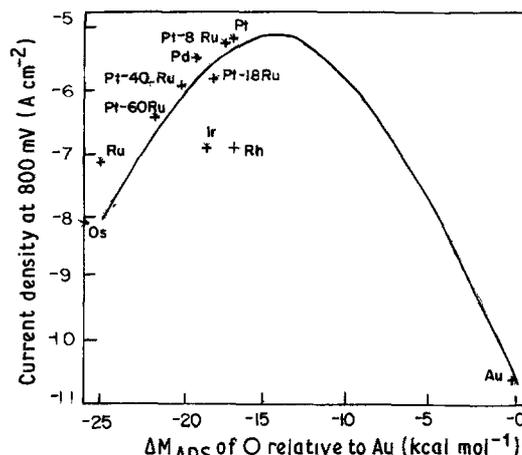
this activity enhancement to structural changes caused by alloying. In 1983, Jalan tried to correlate the alloy catalyst activity as an indirect function of adsorbate bond strength [67, 68]. The function used was bulk interatomic distance in the alloy, which was related to bond tightness and hence to the strength of the HO_2 (a.d.s.) adsorbate bond involved in the rate-determining step for molecular dioxygen reduction $O_2 + H^+ + e^- \longrightarrow HO_2$ (a.d.s.). Jalan's correlation, which can be regarded as a fine tuning of the basic Volcano plot [69] (Fig. 14), is shown in Fig. 15 [67, 68].

Figure 16 shows a composite Volcano plot as a function of the nearest neighbour distance and incorporates data of Figs 14 and 15. Using these Volcano plots, Jalan *et al.* [68] proposed that the distance between the nearest neighbour platinum atoms on the surface of the unalloyed supported catalyst is not ideal for dual site adsorption of O_2 or HO_2. On the other hand, the introduction of alloying components causes lattice contraction and hence reduction in the nearest neighbour distances which in turn brings about a more favourable and optimum Pt–Pt spacing (while maintaining the favourable platinum electronic properties). This was ascribed as the main reason for the higher ORR activity observed.

By contrast, recent work by Glass and Taylor *et al.* [70] present a very different point of view. This study
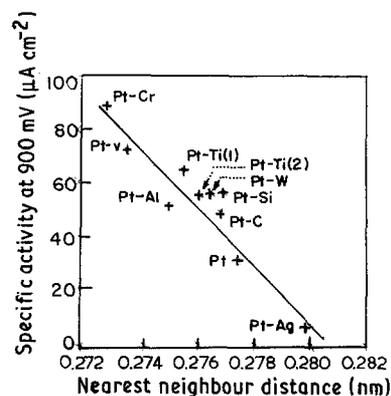

Fig. 15. Correlation of Pt-alloy activity for oxygen reduction in phosphoric acid with nearest neighbour distance (bond strength of reaction intermediates).
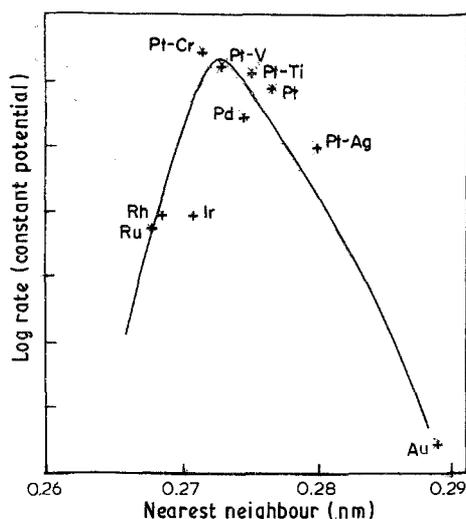
Fig. 16. Composite volcano plot incorporating data from Figs 14 and 15.

Fig. 18. OH coverage at 1.2 V in purified 85 w/o H_3PO_4.

investigated the effect of metallurgical variables (such as varying chromium atom percentage, order disorder transitions in intermetallic and solid solutions, etc.) of the Pt–Cr alloy systems, vis-a-vis their electocatalytic properties (specially the ORR activity). The electrodes were in plane bulk geometric form in contrast to that of gas diffusion geometry used in Jalan's investigation [67, 68]. The results obtained (Fig. 17) were, however, contrary to those of Jalan et al. since no enhancement of electrocatalytic activity for ORR was obtained in Pt–Cr alloys of any composition (ordered alloys giving higher activity vis-a-vis disordered), with 25% chromium ordered samples coming closest in activity to 100% platinum. This is contrary to Jalan's interpretations as lattice contractions do not seem to play any role in the electrocatalytic activity. The explanation advanced by Glass and Taylor et al. [79] has as its basis the data on anodic coverage by OH^- (which follows the same trend as ORR activity), believed to be a one-electron transfer adsorption of OH^- species on to the platinum surface, vis-a-vis atomic percentage of chromium in the binary alloy.

Conway's adsorption model [40] was used to correlate the OH^- monolayer coverage over a 100% platinum (f.c.c.) structure vis-a-vis that on the $\langle 1\,0\,0 \rangle$
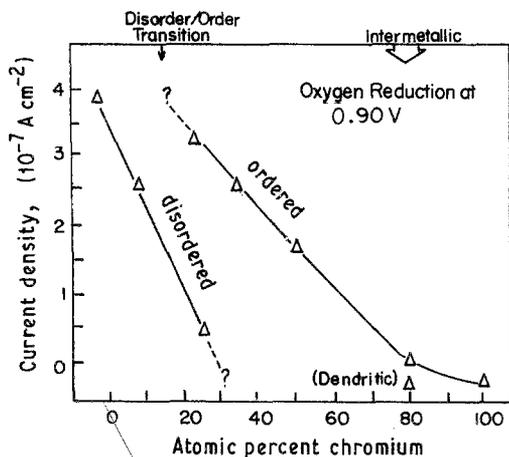
and $\langle 1\,1\,1 \rangle$ faces of an ordered 25% Pt–Cr alloy lattice. This model predicts that at a given potential, 50% of $\langle 1\,0\,0 \rangle$ face and 66% of $\langle 1\,1\,1 \rangle$ face, have a monolayer coverage in a 25% ordered Pt–Cr alloy vis-a-vis that for the same faces in a 100% Pt crystal. This prediction fits the observed data of Glass and Taylor et al. [70] shown in Figs 17 and 18. Extrapolation of Conway's model also predicts coverages on successively smaller fractions of the monolayer with increasing atom % of chromium. However, a quantitative extension of this model to the dioxygen adsorption rate determining step during ORR remains ambiguous. The reason for this is that out of the three identified configurations (Fig. 19) for this oxygen adsorption, only the Pauling end-on configuration (Fig. 19 (a)) [71] is directly analogous to the OH^- case; the others involve more than just a single surface metal atom. However, this configuration had not been totally accepted because end-on geometry predicts higher H_2O_2 formation than that actually observed over purified electrolyte on the platinum surface [72, 73]. The Bridge model [74] (Fig. 19 (b)) and the Griffith model [75] (Fig. 19 (c)) cannot, however, be directly correlated with Conway's model despite the fact that adjacent three-fold geometry of the Griffith model may be better suited to explain the order/disorder property changes in the $\langle 1\,1\,1 \rangle$ plane of a 25% Pt–Cr alloy.

Fig. 17. ORR current density at 0.90 V in purified 85% w/o H_3PO_4.
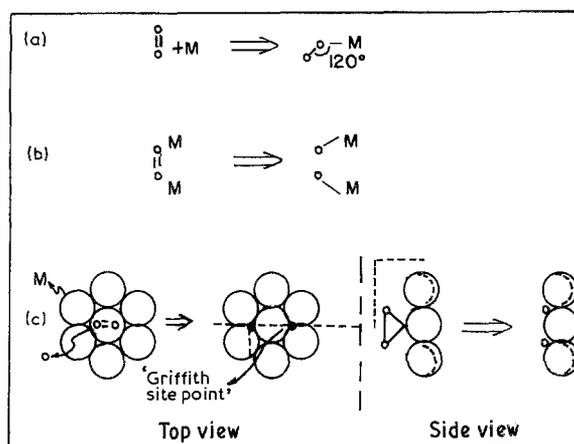

Fig. 19. Probable O_2 adsorption configuration prior to reduction.

Glass and Taylor's indicators towards the independence of lattice parameters on the ORR activity have been supported by studies on a number of bulk platinum alloys in alkaline solution by Giner et al. [76]. The alloys studied include Mn₃ Pt, Mo Pt, Pd Pt, Pt₃ Ti, Pt₃V etc., and are similar to the results of Glass and Taylor et al. [70]. However, none of these alloys were found to have higher activity than 100 a/o Pt, though few were found comparable.

Recent investigations by Paffet et al. [77] provide further insight, by attributing higher ORR activity to be the result of dissolution of the passive alloying component, leading to surface roughening and hence increased surface area. Their results show that potential excursion, especially beyond + 1.25 V with respect to RHE results in selective depletion of chromium (present as Cr (III) oxide or hydroxide on the surface) as Cr (IV) species in solution. The consequent surface roughening and the associated increase in effective platinum surface area is the principal reason causing the observed increment in ORR activity. Binary alloys of PtCr with Cr compositions less than 50% have been shown to produce chromium depletions extending 2–3 monolayers into the surface. The bulk alloys richer in chromium have, however, been shown to suffer from much greater depletion with platinum enriched zone capable of extending up to 100 nm into the surface [78–80].

However, surface roughening does not fully explain the many-fold increase in the initial intrinsic ORR activity, primarily because the operating PAFC potentials are between 0.65 to 0.7 V with respect to RHE which is significantly lower than the passive potential region of (+ 1.25 V with respect to RHE). In addition, these studies have been conducted at room temperature (298 K) with planar bulk geometric electrodes and hence cannot be congruent to the gas diffusion electrode under PAFC conditions.

Hence, the observed activity enhancement for ORR in the gas diffusion electrode geometry could primarily be attributed to factors prevalent in the gas diffusion geometry. This conclusion is corroborated by Ross and Appleby [77] who have surmised two possible options: (a) the oxide formed upon alloying acts as an impediment to platinum crystallite size growth by coalescence (which would decrease ORR activity); (b) the oxide acts as a flux for improving the wettability of the catalysts. These explanations do not seem sufficiently adequate to explain the many-fold increase in catalytic activity of platinum alloys (Pt–V, Pt–Cr) in the gas diffusion electrode geometry [65, 66]. There are also other parameters: (i) Since the rate-determining step of the ORR (formation of [HO₂] a.d.s.) involves both adsorption of molecular dioxygen and the transfer of an electron $O_2 + * + H^* + e^- \longrightarrow [HO_2]$ a.d.s., the configuration of oxygen during adsorption may be important. In the planer bulk geometry and room temperature environment of Glass and Taylor et al. [85] the oxygen adsorption may be rate limiting. In the gas diffusion geometry, however, with temperatures of 150–200° C, only the electron transfer step may be rate

limiting. Furthermore the oxygen adsorption geometry in the two environments may be entirely different. (ii) The particle size and distribution, together with better site time yields (turnover frequency) in gas diffusion electrodes, may have a significant effect in explaining the observed activities.

Besides the parameters discussed above, there may be several other parameters responsible for higher catalytic activity of platinum alloys in gas diffusion electrodes. Hence, for a better understanding, further investigation are required with regard to a definite ORR mechanism and geometry, as well as critical parameters exclusive to the gas diffusion electrode geometry.

5. Conclusions

An overview of particle size and structural correlations to electrocatalytic activity and the fundamental parameters affecting them have been attempted in this review in order to increase general awareness in this area of electrocatalysis and provide broad guidelines for future research. To begin at a fundamental level, attempts in correlating a satisfactory geometric model to the highly dispersed electrocatalyst system have met with very limited success. This is primarily due to the fact that small particles possess structures very different from those at the macroscopic level. The surface stresses and shapes of these small microcrystals give them different properties from those in the bulk. In this context, the microstructure of highly dispersed platinum on carbon support, studied by Jalan et al. [13], provides some new insights: for example, the existence of surface platinum microcrystals (2.0–3.0 nm) as flat platelets is in contrast to spherical shapes assumed for most geometric models. These small microcrystals, with their associated unique surface properties, have a significant effect on catalyst support interactions. A thorough examination of the microstructure of these small microcrystals in 2.0–5.0 nm ranging over a large number of turbostatic carbon blacks is required to give further insight into the actual shapes of these crystallites and their interactions with the carbon support.

Particle size dependence on catalyst-support interactions as suggested by Bogotski et al. [18] needs further study to actually determine the size of the electrical double layer formed between the microdeposit and the support. This would involve an accurate and unambiguous determination of electronic work function of the microdeposit and support materials, and the electrocatalyst under controlled conditions with platinum of different particle sizes.

The two divergent views on the effects of particle size on the anodic hydrogen oxidation reaction, as presented by Vogel et al. [35], Ross and Stonehart et al. [34] and Urrison et al. [37], need to be resolved. Tentatively, the cause of differences in their results can be deduced to differences in pre-treatments of high surface area electrocatalyst particles and the choice of carbon support. The latter, due to its availability in a

wide spectrum of physical, chemical and electronic properties, could have a profound effect on electro-catalytic properties due to differences in electrocatalyst support interactions. However, it would be reasonable to expect some particle size effects because of the presence of a third anodic peak observed between the strongly and weakly adsorbed hydrogen peaks in the anodic potentio-dynamic profiles for hydrogen deposition and oxidation [26, 27]. This third anodic peak varies with particle size and increases with the decrease in particle size (increasing surface area) and accounts for approximately 14% of the total adsorbed hydrogen coverage for a particle size of around 4.2 nm. Hence further quantitative analysis is required to resolve the two divergent views of Vogel and Urrison et al.

The earlier contradictions involving particle size and structural correlation with the oxygen reduction reaction have been somewhat allayed by the recent work of Peuckert et al. [63]. This investigation has also successfully accounted for the results of the earlier research work. Even so, further research efforts are required to establish the various dioxygen adsorption geometries on these highly dispersed electrocatalysts and also to establish a definitive oxygen reduction reaction mechanism. In addition, the exact reasons for catalytic enhancement caused by alloying has yet to be resolved: for this, a detailed model of a porous gas diffusion electrode geometry is required.

Acknowledgement

References

[1]   R. V. Hardeveld and A. V. Montfoort, Surf. Sci. 4 (1969) 396.
[2]   K. Kinoshita, 'Modern Aspects of Electrochemistry', vol. 14, Plenum. New York (1983).
[3]   K. Kinoshita and P. Stonehart, ibid. vol. 12 (1977) p. 183.
[4]   H. Knozinger, Adv. Catal. 25 (1976) 185.
[5]   T. C. Gonzalez, K. Aska, S. Namba and J. Turkevich, J. Phys. Chem. 66 (1962) 48.
[6]   H. L. Gruber, J. Phys. Chem. 66 (1962) 48.
[7]   O. M. Poltorak and V. S. Boronin, Russ. J. Phys. Chem. (Eng. transl.) 39 (1965) 1329, 40 (1966) 1436.
[8]   R. Hardeveld and F. Hartog, Proc. Int. Congr. Catal.; 4th, paper no. 70 (1968).
[9]   P. N. Ross Jr., J. Electrochem. Soc. 126 (1979) 67.
[10] V. M. Jalan and C. L. Bushnell, U.S. Patent 4,136,056 and 4,137,373 (23 Jan. 1979).
[11] V. M. Jalan, 'Preparation of highly dispersed platinum and its stabilization by carbon'. Meeting of Electrochem. Society, Montreal, Canada (9–14 May 1982).
[12] A. Pebler, J. Electrochem Soc. 133 (1) (1986) 9.
[13] V. M. Jalan, Microstructure of highly dispersed Pt catalyst and its interaction with carbon supports, Workshop on Oxygen Electrochemistry', Quail Hollow, Painesville, Ohio (2–4 May 1979).
[14] L. J. Hillenbrand and J. W. Lacksonen, J. Electrochem. Soc. 112 (1965) 249.
[15] J. Escard, C. Leclerc and J. P. Contour, J. Catal. 29 (1973) 31.
[16] V. S. Bogotski and A. M. Snudkin, Electrochemica Acta 29

[17] A. V. Kobelev, R. M. Kobeleva and V. F. Ukhov, Dokl. Akad. Nank. (USSR) 243 (1978) 692.
[18] M. W. Brieter, 'Electrochemical Processes in Fuel Cells. Springer-Verlag, Berlin and New York (1969).
[19] R. Woods Jr., Electroanal. Chem. 49 (1974) 217.
[20] P. N. Ross Jr., in "Electrocatalysis of Fuel Cell Reactions", Brookhaven Natl. Lab., Upton, New York (1978) p. 169.
[21] M. Bold and M. Brieter, J. Electrochem. 64 (1970) 897.
[22] L. Vertzh, I. A. Mosevich and I. Tverdovsky, Dokl. Akad. Nank. (SSSR) 140 (1961) 149.
[23] P. N. Ross Jr., Electroanal. Chem. 76 (1977) 139.
[24] F. G. Will, J. Electrochem. Soc. 112 (1965) 451.
[25] G. C. Bond, Catalysis by Metals, Academic Press, New York (1962) pp. 162–170.
[26] K. Kinoshita, J. Lundquist and P. Stonehart, J. Catal. 31 (1973) 325.
[27] K. Kinoshita and P. Stonehart, Electrochem Acta 23 (1978) 45.
[28] H. Angerstein-Kozlowska, W. B. A. Sharp and B. E. Conway, in Proceedings of the Symposium on Electro-catalysis. (edited by M. W. Brieter), Electrochemical Society, Princeton, New Jersey (1974) p. 94.
[29] A. Damjanovic, A. Dey and J. O'M. Bokris, J. Electro-chem. Soc. 113 (1966) 739.
[30] W. E. O'Grady, M. Y. C. Woo, P. L. Haggans and E. Yeager, in Proceedings of the Symposium on Electrode Materials and Processes for Energy Conversion and Storage (edited by J. D. E. McIntyre, S. Srinivasan and F. G. Will), Electrochemical Society, Princeton, New Jersey (1977) p. 172.
[31] E. Yeager, W. E. O'Grady, M. Y. C. Woo and P. Haggans, J. Electrochem. Soc. 125 (1978) 348.
[32] A. T. Hubbard, R. M. Ishikawa and J. Kate-Karu, J. Electroanal. Chem. 86 (1978) 271.
[33] D. Shopov, A. Andreev and D. Petkov, J. Catal. 1 (1969) 123.
[34] P. Stonehart and P. N. Ross, Catal. Rev. Sci. Eng. 12 (1975) 1.
[35] W. Vogel, J. Lundquist, P. N. Ross and P. Stonehart, Electrochim Acta 20 (1975) 79–93.
[36] P. N. Ross and P. Stonehart, J. Res. Inst. Catal. (Hokkaido) 22 (1974) 22.
[37] N. A. Urrison, G. V. Shtienburg and V. S. Bogotski, Electrokhimiya 11 (1975) 1298.
[38] M. A. Barett and R. Parson, J. Electroanal. Chem. 42 (1975) App. 1.
[39] B. E. Conway and S. Grottesfield, J. Chem. Soc. Faraday Trans. 1. 69 (1973) 1090.
[40] H. Angerstein-Kozlowska, B. E. Conway and W. B. A. Sharp, J. Electroanal. Chem. 43 (1973) 9.
[41] B. V. Tilac, B. E. Conway and H. Angerstein-Kozlowska, J. Electroanal. Chem. 48 (1973) 1.
[42] D. A. J. Rand and R. Woods, J. Electroanal. Chem. 31 (1971) 29.
[43] R. Parsons and W. H. M. Visscher, J. Electroanal. Chem. 36 (1972) 329.
[44] K. J. Vetter and J. W. Schultze, J. Electroanal. Chem. 34 (1971) 131, 141.
[45] T. Biegler and R. Woods, J. Electroanal. Chem. 20 (1969) 73.
[46] K. S. Kim, N. Wingorad and R. E. David, J. Am. Chem. Soc. 93 (1971) 6296.
[47] K. S. Kim, A. F. Gossman and N. Wingorad, Anal. Chem. 46 (1974) 197.
[48] A. K. N. Reddy, M. A. Genshaw and J. O'M. Bokris, J. Chem. Phys. 48 (1968) 671.
[49] S. Gillman, Electrochim Acta 9 (1964) 1025.
[50] R. Ducros and R. P. Merrill, Surf. Sci. 55 (1976) 227.
[51] P. Le'gar'e, G. Maire, B. Carriere and J. P. Deville, Surf. Sci. 68 (1977) 348.
[52] A. Damjanovic and V. Brusic, Electrochim Acta 11 (1967) 615.
[53] A. J. Appleby, J. Electrochem. Soc. 117 (1970) 328.
[54] A. Damjanovic, M. A. Genshaw and J. O'M. Bokris, J. Electrochem. Soc. 114 (1967) 466, 1107.
[55] P. N. Ross Jr., J. Electrochem. Soc. 126 (1979) 78.
[56] A. J. Appleby and B. S. Baker, J. Electrochem. Soc. 125 (1978) 404.
[57] H. Zeliger, J. Electrochem. Soc. 114 (1967) 144.
[58] J. Bett, J. Lundquist, E. Washington and P. Stonehart,

(5) (1984) 757–67.

Electrochim Acta. **18** (1973) 343.

[59] H. R. Kunz and G. A. Gruver, *J. Electrochem. Soc.* **112** (1975) 1279.

[60] W. M. Vogel and J. M. Baris, *Electrochem Acta* **22** (1977) 1259.

[61] K. F. Blurton, P. Greenburg, G. H. Oswin and D. R. Rutt, *J. Electrochem. Soc.* **119** (1972) 559.

[62] L. J. Bregoli, *Electrochim. Acta* **23** (1978) 489.

[63] M. Peuckert, T. Yoneda, R. A. Dalla Betta and M. Boudart, *J. Electrochem. Soc.* **113** (5) (1986) 944–947.

[64] P. N. Ross, Electric Power Research Institute *EPRI-EM-1553; EPRI,* Palo Alto, CA. (1980).

[65] V. M. Jalan and D. A. Landsman, U.S. Patent 4,186,110 (29 Jan. 1980); V. M. Jalan, D. A. Landsman and J. M. Lee, U.S. Patent 4,192,907 (11 March 1980); V. M. Jalan, U.S. Patent 4,202,934 (13 May 1980).

[66] D. A. Landsman and F. J. Luczak, U.S. Patent 4,136,944 (23 Feb. 1982) and 4,373,014 (18 Feb. 1983).

[67] V. M. Jalan and E. J. Taylor, *J. Electrochem. Soc.* **130** (1983) 2299.

[68] V. M. Jalan and E. J. Taylor, *Proceedings of the Symposium on the Chemistry and Physics of Electrocatalysis,* vol. 84 (12). The Electrochemical Society, (1984) pp. 547–57.

[69] A. J. Appleby, *Cat. Rev.* **4** (2) (1970) 221.

[70] J. T. Glass, G. L. Cahen and G. E. Stoner, *J. Electrochem. Soc.* **134** (1987) 58–65.

[71] L. Pauling, *Nature* **203** (1964) 182.

[72] J. P. Hoare, in 'Advances in Electrochemistry and Electro-

Chemical Engineering' vol. 6. (edited by P. Delahay) Interscience, New York (1967) p. 201.

[73] E. Yeager, D. Scherson and B. Simic-Glavasky, in 'The Chemistry and Physics of Electrocatalysis', (edited by J. D. E. McIntyre, M. J.Weaver and E. B. Yeager), The Electrochemical Society Softbound Proceedings Series, Pennington, N.J. (1984) p. 247.

[74] E. Yeager, in "Electrode Materials and Processes for Energy Conversion and Storage" (edited by J. D. E McIntyre, S. Srinvasan and F. G. Will), The Electro-Chemical Society Softbound Proceedings Series, Princeton N.J. (1977) p. 149.

[75] J. L. Gland, B. A. Sertin and G. B. Fisher, *Surf. Sci.* **95** (1980) 587.

[76] J. Giner, J. Parry, L. Sweette and R. Catabriga, prepared for the National Aeronautics and Space Administration, Contract No. NASW-1233 (June 1968).

[77] P. N. Ross and A. J. Appleby, *Personal Communication* (1984).

[78] M. T. Paffett. J. G. Beery and G. Shimshon, *J. Electrochem. Soc.* **135** (6) (June 1988) 1431.

[79] K. A. Daube, S. Paffett, S. Gottesfield and C. T. Compbell, *J. Vac. Sci. Technol.* **a, 4** (1986) 1617.

[80] M. T. Paffett, K. A. Daube, S. Gottesfeld and C. T. Compbell, *J. Electroanal. Chem. Interfacial Electrochem.* **220** (1987) 269.

[81] S. Gottesfeld, M. T. Paffett and A. J. Reodondo, *Electroanal. Chem. Interfacial Electrochem* **43** (1988) 9.